

1 **Development of conductive cementitious materials using recycled carbon fibres**

2

3 G. Faneca^a, I. Segura^{b, c*}, J. M. Torrents^d, and A. Aguado^b

4

5 ^a Escofet 1886 Ltd.

6 ^b Department of Construction Engineering, Universitat Politècnica de Catalunya - Barcelona

7 Tech, C1, Barcelona 08034, Spain

8 ^c Smart Engineering Ltd., C/Jordi Girona 1-3, Parc UPC – K2M, Barcelona 08034, Spain

9 ^d Department of Electronics Engineering, Universitat Politècnica de Catalunya - Barcelona

10 Tech, C4, Barcelona 08034, Spain

11

12 **Abstract**

13 Conductive cementitious materials have gained immense attention in recent years owing to

14 the possibility of achieving multifunctional materials. The usual approach has been to

15 incorporate carbonaceous nanomaterials and/or virgin carbon fibres into cementitious

16 matrices. This paper presents the first research devoted to the development of conductive

17 cementitious materials using recycled carbon fibres (rCFs). Four different types of PAN-

18 based rCFs were studied, by varying the aspect ratio and supplying characteristics, in two

19 concrete dosages: conventional and ultra-high-performance concrete mixes. Two mixing

20 methods—dry and wet—commonly used to fabricate fibre-reinforced concrete were

21 considered. The results obtained in our result have shown that wet mix method achieves better

* Corresponding author: Ignacio Segura Pérez. Universitat Politècnica de Catalunya. Departament d'Enginyeria de la Construcció. Carrer Jordi Girona 1-3, Edificio C1, despacho 202. E-08034 Barcelona. SPAIN. Email:

ignacio.segura@upc.edu. Tel.: +34-93-401-65-30. Fax: +34-93-405-41-35

22 workability of the mixes and good dispersion of the fibres. Furthermore, electrical resistivity
23 values in the range of 3–0.6 $\Omega\cdot\text{m}$ were obtained for rCF contents ranging from 0.2 to 0.8% in
24 vol. The obtained results demonstrate the possibility of using rCF to develop multifunctional
25 cementitious materials and thus enhance the possibility of using these materials from an
26 industrial point of view. Furthermore, new possibilities are created for the recycling of carbon
27 fibre composites to obtain high-added-value products.

28

29 **Keywords**

30 Conductive concrete; Recycled carbon fibre; smart cementitious materials

31

32 **1. Introduction**

33 Concrete is currently the most widely used construction material and is likely to remain the
34 predominant material in the near future. It forms an integral part of global civil infrastructures,
35 ranging from small buildings to large structures such as tunnels, long-span bridges, and offshore
36 platforms. Moreover, most of the current infrastructure in the developed world is past its
37 designed service-life. One in three railway bridges in Germany is more than 100 years old, as
38 are half of London's water mains. In America, the average bridge is 42 years old and the average
39 dam is 52 years old. The American Society of Civil Engineers rates approximately 14,000 of
40 the country's dams as 'high hazard' and 151,238 of its bridges as 'deficient' (1). The European
41 Innovation Partnership on Smart Cities and Communities (EIPSCC) evaluated key urban
42 infrastructure and most cities were described as 'aged and stressed' (2).

43

44 As most of Europe's infrastructure is already built, in the near future, efforts must be made to
45 enhance the safety, efficiency, energy consumption, structural performance, and sustainability
46 of new and existing buildings and infrastructure. A way forward to overcome the

47 aforementioned problems could be the use of smart, multifunctional construction materials. The
48 term ‘multifunction’ was coined to highlight the ability of a material to simultaneously exhibit
49 specific desirable electronic, magnetic, optical, thermal, or other properties to satisfy previously
50 unattainable performance metrics (3). The development of smart materials and infrastructure is
51 a hot research topic and an interesting focus for public opinion. Recently, energy-harvesting
52 tiles were used during the Paris marathon of 2013 and helped to produce 4.7 kWh of energy
53 (4). Current research trends in smart cementitious materials include self-healing concrete (5,6),
54 enhanced bioreceptivity concrete (7,8), mortars with biocide characteristics (9), and
55 development of conductive cementitious materials.

56

57 The incorporation of conductive phases into cementitious matrices has been one of the most
58 popular methodologies to obtain conductive and thus multifunctional cementitious materials.
59 The early works of Chung et al. (10–13) demonstrated the possibility of developing
60 multifunctional cementitious materials by adding carbon fibres into concrete. Several studies
61 have considered this path and it is still a topic of interest. The incorporation of carbonaceous
62 materials (carbon fibres, carbon black, and carbon nanomaterials) into cement-based materials
63 has achieved a wide range of novel functionalities. Apart from self-sensing capabilities (14–
64 18), such an approach has resulted in cementitious materials with other properties, such as
65 electromagnetic shielding (19,20), self-heating (17,21–23), cathodic protection of structures
66 (24,25), and chloride removal (25,26).

67

68 Conductive cementitious materials can be obtained by incorporating different type of
69 functional materials. Han et al (27) identified up to ten different functional materials that have
70 been used up to date to develop conductive multifunctional cementitious materials, including
71 shortcut carbon fibres (CF), carbon nanotubes and nanofibers (CNT/CNF), carbon black, steel

72 slag, and steel fibres. The use of steel fibres presents a high potential to develop conductive
73 cementitious materials, i.e. for de-icing applications (28), since they are actually been widely
74 used in the civil engineering industry as sole reinforcement in structural concrete applications.
75 However, there are some drawbacks about using steel fibres to develop multifunctional
76 cementitious materials, since the applied current may promote the corrosion of the fibres.
77 Thus, carbon products were used to replace steel shavings in the conductive cementitious
78 materials mixture design (17). Among all functional materials used up-to-date, cementitious
79 matrices with either chopped CF and CNT/CNF are the most extensively and
80 comprehensively studied in the literature (27). More recently, other authors have also been
81 considered the utilisation of graphene mixed with other carbonaceous materials to develop
82 self-sensing cementitious materials (29). Along with the laboratory scale studies, there are
83 some examples of real scale use of conductive cementitious materials in the literature. One of
84 the first works was presented by Tuan in 2008 (28), using a mix of carbonaceous materials
85 and steel fibres. Most of the real-scale tests were intended for de-icing applications (21,30),
86 and for self-sensing applications (15). However, we are still far away to find multifunctional
87 cementitious materials fully incorporated into the civil engineering industry. Recently some
88 efforts have been made to commercialise chopped carbon fibre but the costs are significantly
89 higher than those of other fibres used in the civil engineering industry. A possible way to
90 achieve low-cost multifunctional cementitious materials is the use of recycled carbon fibres
91 (rCF). Recycled carbon fibres are mainly obtained from aerospace composite scrap. Among
92 many different methods, most of the commercially available rCF are obtained via pyrolysis.
93 This process allow a high retention (up to 90%) of the properties exhibited by virgin carbon
94 fibres (31,32). The use of this kind of fibres in cementitious materials has gained attention last
95 years, as more companies have started worldwide to provide rCF in a commercial way. Most

96 of recycling processes yield rCF with high retention of mechanical properties (33) but with a
97 30 to 40 percent cost savings versus virgin carbon fibre.

98

99 The objective of this article is to evaluate the effect of different rCFs on the mechanical and
100 electrical properties of cementitious materials. Accordingly, different types of rCFs were
101 added with different contents (0.1 to 1.4% in volume) to conventional concrete (CC) and
102 ultra-high-performance concrete (UHPC) dosages. The effect of the incorporation of rCF on
103 the slump flow was evaluated. Furthermore, compressive and flexural strength measurements
104 were obtained in concrete samples along with electrical measurements. Finally, rCF
105 dispersion was evaluated via visual inspection.

106

107 **2. Research significance**

108 This study is the first research devoted to the development of conductive cementitious
109 materials using rCF. Other researchers have studied the incorporation of rCF into polymeric
110 matrices and evaluated their mechanical and electrical properties (34–36). Only the recent
111 work by Nguyen et al. has evaluated the effect of these kinds of fibres on the mechanical
112 properties of cementitious materials, but the rCFs used were reclaimed carbon fibres that were
113 not treated to eliminate polymer residue (37,38). The main aim of this study is to provide
114 insights into the use of rCF as a conductive phase to develop multifunctional cementitious
115 materials. The research outcome might facilitate the development of novel multifunctional
116 cementitious materials that can be employed in the civil engineering industry and thus modify
117 the actual paradigm of our structures.

118

119 **3. Materials and methods**

120 **3.1 Concrete mixing proportions and raw materials**

121 Two different concrete mixing proportions were used in our study (see Table 1): a
 122 conventional concrete mix (CC) and an ultra-high-performance concrete mix (UHPC). The
 123 main difference between both mixing proportions is the granular skeleton and cement content
 124 and they were selected to evaluate the possible presence of a double percolation phenomenon.
 125 This phenomenon was firstly described by Wen et al (39) and it involves fibre and cement
 126 paste percolation, as the aggregates might determine the existence of electrical conductivity
 127 through the cement paste. They demonstrated this effect in conductive cementitious materials
 128 as the aggregates might determine the existence of electrical conductivity through the cement
 129 paste. The maximum aggregate size in the UHPC dosage is 1 mm whereas that in the CC
 130 dosage is 12 mm. The water-to-cement ratio (w/c) also differed in both mixes—0.45 in the
 131 CC mix and 0.14 in the UHPC mix.

132

133 Table 1. Concrete mixing proportions for conventional and ultra-high performance mixes

| Component | | Dosage (kg/m ³) | |
|---------------------|----------------|-----------------------------|------|
| | | CC | UHPC |
| Cement | | 400 | 800 |
| Filler | | 260 | 220 |
| Sand (0–3/0–1 mm) | | 500 | 1161 |
| Pea gravel (2–4 mm) | | 520 | -- |
| Gravel (4–12 mm) | | 400 | -- |
| Additives | Glenium B255 | 16 | -- |
| | Glenium ACE425 | -- | 30 |
| | Meyco MS685 | -- | 57 |
| Water | | 180 | 110 |

134

135 The cement selected to produce different mixtures was CEM I 53.5R. Filler was incorporated
 136 into the different dosages to achieve an optimum workability of the mixes with a low
 137 consumption of superplasticisers. The aggregates used for the CC mix were all granite and the
 138 filler was marble dust. The sand used for the UHPC mix was siliceous sand and the filler was

139 calcium carbonate (Betoflow). A polycarboxylate superplasticiser (Glenium B225) was used
 140 for the CC mix and the UHPC dosage used both a polycarboxylate superplasticiser (Glenium
 141 ACE425) and nanosilica suspension (Meyco MS685) to provide self-compacting
 142 characteristics to the concrete mix.

143

144 **3.2 Recycled carbon fibres**

145 The rCFs evaluated were PAN-based carbon fibres in all cases. The rCFs were provided by
 146 ELG Carbon Fibre Ltd. (CFRAN, C10/30, and CT12) and CAR FiberTec (CFTrim). The
 147 characteristics of all the rCFs are listed in Table 2. CFRAN and C10/30 are monofilament
 148 rCFs differing in their average length; CT12 and CFTrim are fibrillated sheets. The fibre
 149 factor, F , illustrates the effect of both the volume fraction and geometrical characteristics of
 150 the fibres and was first proposed by Narayanan and Darwish (40) as equation [1]:

$$151 \quad F = \beta \cdot V_f \cdot L_f / d_f \quad [1]$$

152 where β is the fibre shape factor (0.50 for round fibres), V_f is the volume fraction of fibres,
 153 and L_f and d_f are the length and diameter of the fibre, respectively (L_f / d_f : fibre aspect ratio).

154 Both the fibre factor and mix design determine the maximum concentration of fibres in a
 155 given concrete dosage. The fibre dosage varied from 0.1% to 1.4% in volume.

156

157 Table 2. Properties of recycled carbon fibres as given by the suppliers

| Property | Value | | | |
|----------------------------------------------------|--------------------------|--------|----------------|--------|
| | CFRAN | C10/30 | CT12 | CFTrim |
| Diameter (μm) | 7.5 | | 7 [†] | |
| Nominal length (mm) | 6 - 60 | 10-30 | 12 | 12 |
| Average length (mm) | 40 | 20 | 12 | 12 |
| Density (kg/m^3) | 1800 | | | 1760 |
| Tensile strength (MPa) | 3150 | | 4150 | 4200 |
| Young modulus (GPa) | 200 | | 252 | 240 |
| Electrical resistivity ($\Omega \cdot \text{m}$) | 0.103/0.34 ^{††} | | | 0.016 |

| | | | |
|------------------|------------------|------------------|----------------|
| Fibre factor (-) | $4286 \cdot V_f$ | $1428 \cdot V_f$ | $12 \cdot V_f$ |
|------------------|------------------|------------------|----------------|

158
159
160

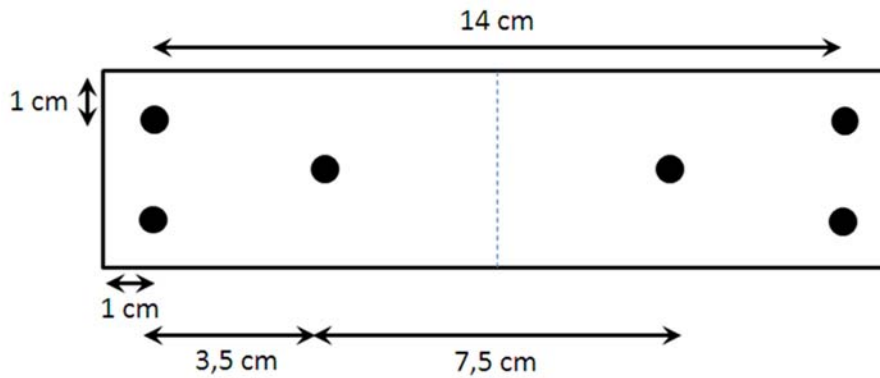
† The effective diameter of the fibrillated sheets is 500 μm .

†† The electrical resistivity varies if the measurement is made lengthways (0.103) or across the cross-section (0.34)

161 3.3 Sample fabrication

162 Several methods, varying in complexity, are described in the literature to disperse carbon
163 fibres into cementitious matrices, although most of them are significantly different from the
164 normal practice. In this study, concrete samples were intended to be produced using a
165 fabrication procedure as close as possible to the industrial processes. Thus, the different
166 concrete mixes were fabricated at the industrial installations of the company Escofet 1886.
167 Specimens with dimensions 40x40x160 mm were fabricated from the mixes indicated in
168 Table 1 according to UNE-EN 196-1 (41). Two sets of samples were fabricated from each
169 mix—one for the mechanical measurements and the other for the electrical measurements.
170 The dispersion of carbon fibres is one of the most critical issues in the fabrication of carbon
171 fibre-reinforced cementitious materials. Many different methods are available in the literature,
172 ranging from the surface modification of the carbon fibres, the incorporation of different
173 admixtures (methylcellulose, water reducing agents, etc.), to the use of physical methods as
174 ultrasonic sonication (27,42). Our aim was to work as close as possible to the real practice and
175 the actual concrete compositions used in the precast concrete industry. In this work, rCFs
176 were added to the mix using two methods normally used by the construction industry to
177 manufacture fibre-reinforced cementitious materials: in the dry mix (D) after incorporating
178 the cement and aggregates and in the wet mix (W) after incorporating the water and additives.
179 Furthermore, reference samples were obtained with no addition of rCF. The electrodes used
180 for the electrical measurements were stainless steel set screws of length 5 cm, which were
181 dipped 3.5 cm into the concrete samples. Figure 1 shows a scheme on the electrodes
182 positioning on the specimens.

183



184

185 Figure 1. Location of the electrodes in the specimens

186

187 The samples were cured in a curing chamber ($20^{\circ} \pm 2^{\circ}\text{C}$; $95 \pm 5\%$ relative humidity) for 28
 188 days. The sample notation was carried out according to the following code: CC/U
 189 distinguishes between CC and UHPC (denoted as U) mixes, C_f indicates the fibre content
 190 (varying from 00 for the reference sample to 14 for the sample with 1.4% fibre content), f
 191 indicates the fibre type, and M indicates the mixing method of the fibres (D or W).

$$192 \quad \{CC/U\} - C_f - f - M$$

193

194 3.4 Characterisation methods

195 The slump flow was measured according to UNE-EN 1015-3 (44) prior to the elaboration of
 196 the specimens for all the mixes except CFRAN fibres. Flexural and compressive strength
 197 measurements were obtained in the concrete samples according to UNE-EN 196-1 (41); three
 198 and six replicates were made for each dosage. The electrical characterisation of the samples
 199 was performed using an Agilent HP 4192A impedance analyser and using an instrumentation
 200 amplifier as the front-end to allow 4-probe measurements (45) with an effective voltage of 1
 201 V AC to avoid polarisation effects in the electrodes (46,47). The measurements were obtained
 202 with the frequency scanning from 10 Hz to 1 MHz, providing electrical impedance (Z , in Ω)
 203 and phase (ϕ , in $^{\circ}$). The electrical impedance is described by equation [2] and is composed of

204 a real part (electrical resistance, R) and an imaginary part (reactance, X). R and X are obtained
205 from equations [3] and [4]:

$$206 \quad Z = R + j \cdot X \quad [2]$$

$$207 \quad R = Z \cdot \cos\left(\frac{\phi \cdot \pi}{180}\right) \quad [3]$$

$$208 \quad X = Z \cdot \sin\left(\frac{\phi \cdot \pi}{180}\right) \quad [4]$$

209 Finally, the electrical resistivity (ρ , in $\Omega \cdot \text{m}$) is obtained using equation [5]:

$$210 \quad \rho = R \frac{S}{l} \quad [5]$$

211 where S is the effective transverse section (0.0016 m^2 in our study) and l is the measurement
212 length (0.07 m in our study). All the samples were allowed to reach hygrothermal equilibrium
213 by maintaining them under laboratory conditions for 15 days after the completion of the
214 curing period. The rCF dispersion in the cementitious matrix was evaluated by visual
215 inspection.

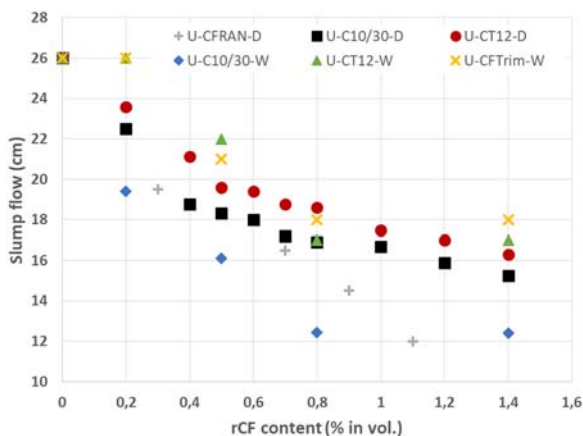
216

217 **4. Results**

218 **4.1 Physical and mechanical properties**

219 The slump flow variation evaluated for different rCFs is shown in Figure 2. The slump flow
220 was not measured in the CC-CFRAN-D samples owing to the difficulties observed during the
221 mixing of the samples. The excess length of this rCF (which was larger than the maximum
222 size of 60 mm provided by the supplier) and the characteristics of the concrete dosage
223 resulted in a significant reduction in the mix workability. The data were grouped into two sets
224 according to the mixing method. The samples with the rCF incorporated into the wet mix (W
225 samples) exhibited slightly larger slump flow for different fibre contents. Furthermore, the
226 rCFs provided as fibrillated sheets (CT12 and CAR) exhibited larger slump flow and thus

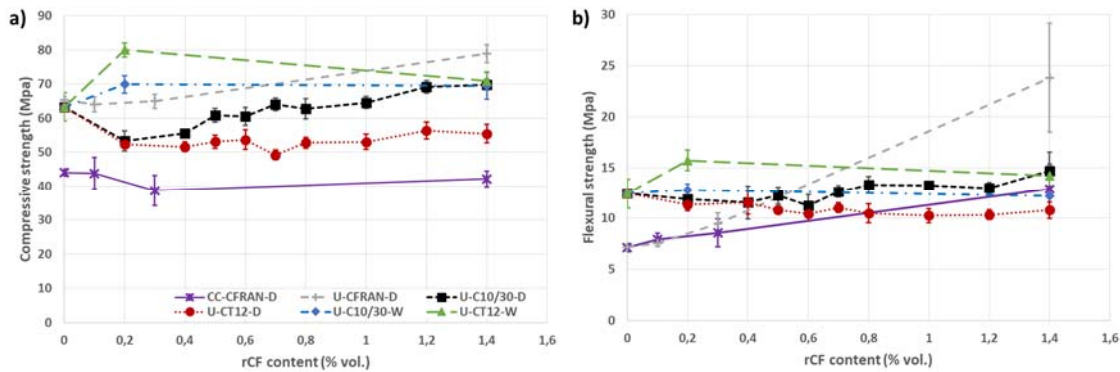
227 better dispersion of the fibres in the cementitious matrix than those presented as single fibres
 228 (CFRAN and C10/30). For all the samples, it was observed that the slump flow was reduced
 229 as the content of rCF was increased, which is consistent with the results presented in other
 230 studies with virgin carbon fibres, although the mixing methods were different (16,48).
 231 Considering the difficulties observed during the fabrication of the conventional concrete
 232 mixes for CFRAN carbon fibres, the rest of the mixes were obtained only with the UHPC
 233 mix. The fibre factor F of the different rCFs, as detailed in Table 2, influences the workability
 234 of the mixes. There are no reported values of the fibre factor in the literature, although
 235 Grunewald provided maximum values between 0.3 and 1.9 for steel-fibre-reinforced concrete
 236 (49). Considering only the rCF characteristics and volume fractions, the fibre factor F varies
 237 between 428 and 6000 for CFRAN, 143 and 2000 for C10/30, and 1.2 and 16.8 for CT12 and
 238 CFTrim.
 239



240
 241 Figure 2. Variation of slump flow with the content of rCF for different mixes

242
 243 The results of the compressive and flexural strength measurements (Figure 3a and b,
 244 respectively) showed different behaviours of the rCF concrete samples. First, concretes made
 245 with CFRAN carbon fibres exhibited a clear influence of the granular skeleton as UHPC
 246 concretes exhibited larger mechanical properties than the CC concretes. As mentioned

247 previously, the incorporation of CFRAN fibres into the conventional concrete mixes resulted
 248 in a large reduction in the workability. The difficulty in mixing the CC dosages influenced the
 249 compaction of the samples and thus, more porosity was incorporated into the mix.
 250 Therefore, these samples exhibited lower mechanical performance. Second, the mixes that
 251 incorporated rCFs into the wet mix exhibited larger compressive strength than the dry mix
 252 samples. This result is also consistent with the results of workability and those of previously
 253 published research works (43)
 254



255
 256 Figure 3. Variation of a) compressive and b) flexural strength with the rCF content for
 257 different mixes

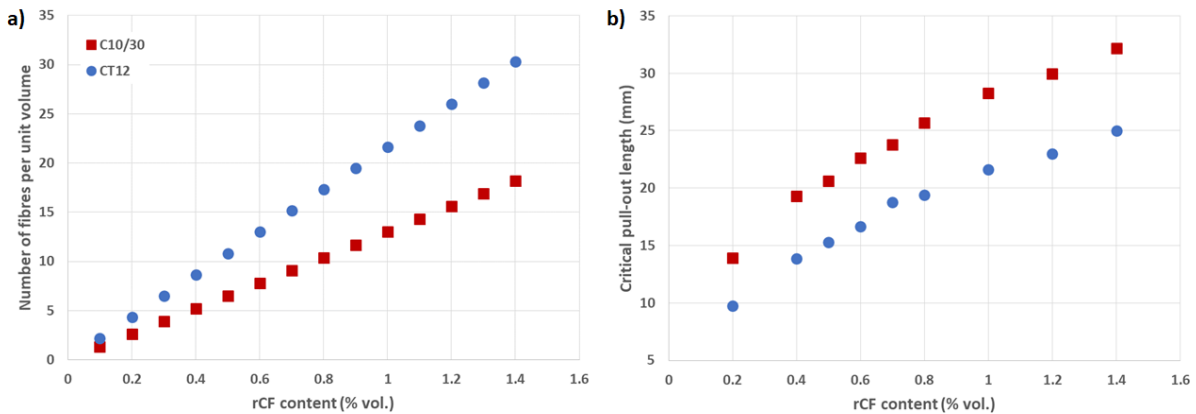
258
 259 Finally, regarding the format of the rCF (single fibre or fibrillated sheets) and considering the
 260 slump test results, larger mechanical response of CT12 samples is expected. Further, when the
 261 rCFs were incorporated into the dry mix, C10/30 samples exhibited larger mechanical
 262 response both in compressive and flexural strength measurements. When the rCFs were
 263 incorporated into the wet mix, the trend shifted and CT12 samples exhibited larger
 264 compressive and flexural strength. This result might be explained in view of the critical pull-
 265 out length (L_f^{crit}) and number of fibres per unit volume (N), as recently presented by Han et al.
 266 (50). In that work, critical pull-out length of carbon fibres can be got when the carbon fibres

267 are snapped. The authors demonstrated that, as the length of the carbon fibre decreases, N
 268 increases but L_f^{crit} decreases.

269

270 Figure 4 presents the variation of N and L_f^{crit} with the rCF content for C10/30 and CT12
 271 fibres. More carbon fibres in the bulk matrix indicate better mechanical performance up to a
 272 certain rCF content given by the fibre factor. Once this value is reached, a further increase in
 273 the carbon fibre content might have a weakening effect owing to the presence of air voids and
 274 low dispersion of the carbon fibres. Thus, N mainly influences the compressive strength. As
 275 shown in Figure 3a, C10/30 and CT12 samples exhibit almost similar compressive strength
 276 for low rCF content, because the number of fibres per unit volume is very similar (see Figure
 277 4a). As the rCF content increases, the difference between N of C10/30 and CT12 increases,
 278 and thus more defects (air voids and bundles of carbon fibres) might be present in the
 279 cementitious matrix.

280



281

282 Figure 4. Variation of (a) N and (b) L_f^{crit} with the rCF content for C10/30 and CT12 fibres

283

284 Furthermore, the value of L_f^{crit} will determine the mechanical behaviour of the carbon fibre
 285 reinforced cementitious composites. As L_f increases and exceeds L_f^{crit} , the carbon

286 fibre maximum stress also increases until $L_f = L_f^{crit}$. Further increases of L_f are not related to
287 larger increases in the fibre maximum stress since the carbon fibre will be snapped from the
288 cementitious matrix when the material is damaged. The length of both C10/30 and CT12
289 carbon fibres is larger than the value of L_f^{crit} for almost all rCF contents (see Figure 4b).
290 Therefore, no significant differences are expected in the flexural behaviours of the specimens
291 as shown in Figure 3b.

292

293 **4.2 Electrical characterisation**

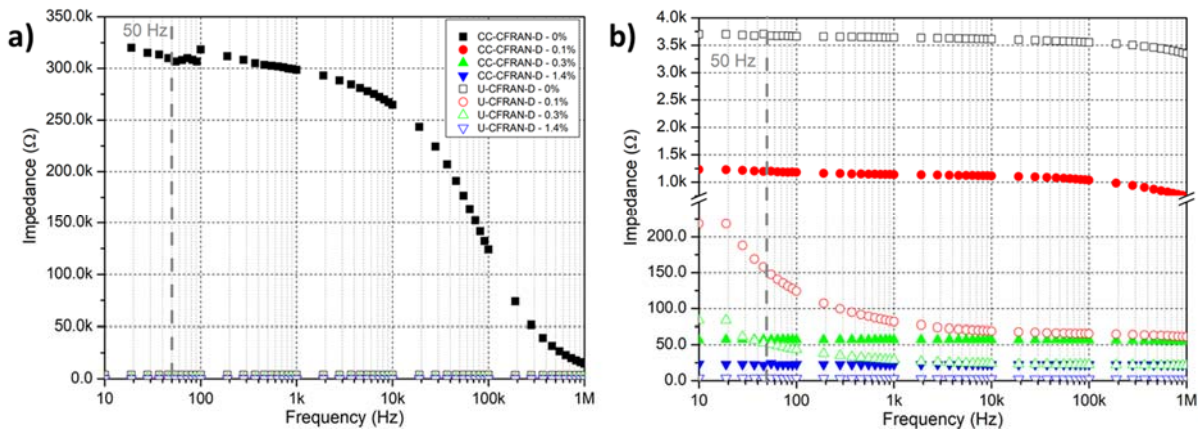
294 **4.2.1 Effect of CFRAN fibres and influence of granular skeleton**

295 First, the influence of the granular skeleton was verified for CFRAN fibre contents of 0.1, 0.3,
296 and 1.4%. The Bode diagrams (impedance versus frequency) for these samples are illustrated
297 in Figure 5. A line is drawn at 50 Hz as it is the standard frequency of electrical mains. The
298 electrical patterns of both CC and UHPC concrete samples exhibit large differences. The plain
299 CC specimens with no rCF addition evidence and impedance variation with frequency
300 characteristic of an insulator material. There is almost no variation of the impedance with the
301 increasing frequency up to 10 kHz. Once this value is reached, a large reduction on the
302 impedance is observed. The plain UHPC concrete samples also behave as an insulator, but the
303 variation of the impedance with frequency is different from the CC samples. Firstly, for the
304 same frequency value, UHPC samples exhibit impedance values that are 100 to 10 times
305 lower than the CC ones; as the frequency increases, the differences between CC and UHPC
306 samples reduces. Secondly, the electrical pattern of the plain UHPC samples do not exhibit a
307 drastic reduction of the impedance for frequency values above 10 kHz, but just a slight
308 reduction in the impedance for frequencies larger than 100 kHz.

309

310 The reduction of impedance observed in the plain CC specimens are related to polarization
 311 effects. Some authors have suggested that polarization effects are not eliminated by the use of
 312 AC but are rather manifested in the form of introduction of a capacitance in parallel with the
 313 electrical resistance. As the frequency of the applied current is increased, the effect of the
 314 capacitance is reduced. The differences observed between the plain concrete samples of both
 315 CC and UHPC mixes are related to the different granular skeletons of the mixes and the
 316 percolation of the cementitious paste (47). The differences between the maximum aggregate
 317 sizes of the CC and UHPC mixes (1 mm in the UHPC mix vs. 15 mm in the CC mix) explain
 318 the different electrical patterns observed. Considering the differences observed in the
 319 electrical behaviour and the difficulties in the mixing process of the CC-CFRAN dosage, only
 320 the UHPC mix was used in the rest of this study.

321



322

323 Figure 5. Bode diagrams for CC and UHPC mixes with CFRAN fibres: a) complete
 324 impedance scale, and b) 0–1300 Ω

325

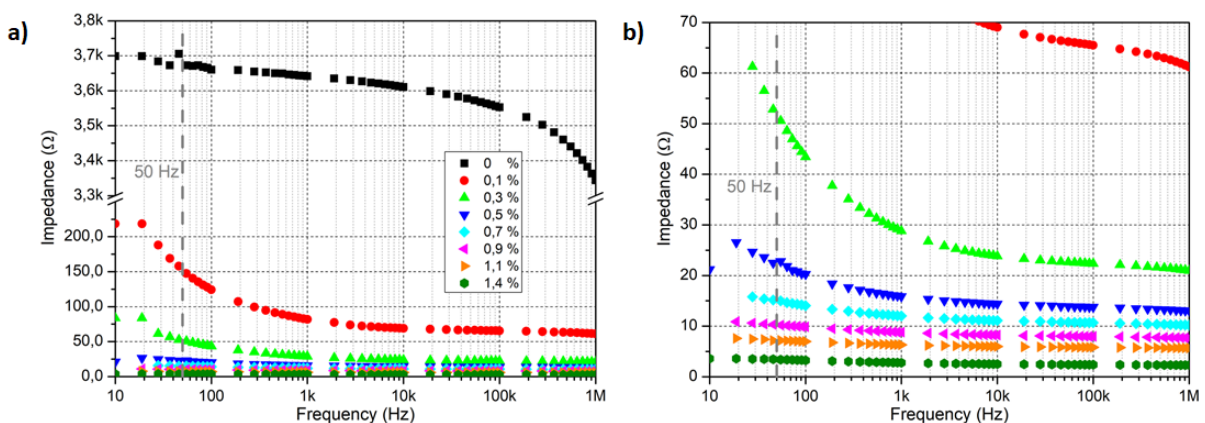
326 Figure 6 shows the Bode diagrams for CFRAN fibre contents from 0 to 1.4% for the UHPC
 327 mix. The incorporation of rCF into the cementitious matrix drastically modifies the electrical
 328 behaviour of the material. The reference samples behave as an insulator with almost no
 329 variation in the impedance with the frequency. A small reduction in the impedance can be

330 observed only for frequencies up to 100 kHz. However, the incorporation of the rCF modifies
 331 the electrical pattern of the samples. It can be observed that the impedance is reduced as the
 332 frequency of the applied current is increased. Large reductions in the impedance values are
 333 observed as the frequency is increased up to 1–10 kHz such that the plateau appears in
 334 accordance with previous studies (51). This frequency helps overcome the effects appearing
 335 in the samples owing to the ionic conductivity of the cementitious matrix, and is referred to as
 336 the *capacitance threshold* (C_t).

337

338 Second, the incorporation of the CFRAN fibres drastically reduces the impedance of the
 339 samples up to the rCF content of 0.6%. Further increments in the CFRAN content do not lead
 340 to larger decreases in the electrical impedance. This electrical behaviour may demonstrate a
 341 continuous electrical path between the electrodes. The visual inspection of the fracture
 342 interfaces of the CC and UHPC concrete samples (see Figure 7) shows that CFRAN fibres
 343 tend to form bunches after mixing. The characteristics of these fibres (very high aspect ratio
 344 and supplying characteristics) did not allow good dispersion of the fibres with the standard
 345 mixing procedures used by the industry.

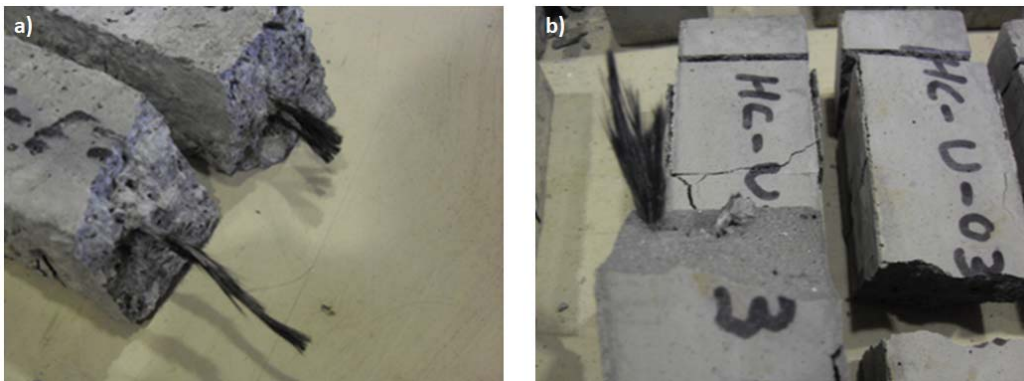
346



347

348 Figure 6. Bode diagrams for UHPC mixes with CFRAN fibres: a) complete impedance scale,
 349 and b) zoom-in the 0–70 Ω range of impedance

350



351

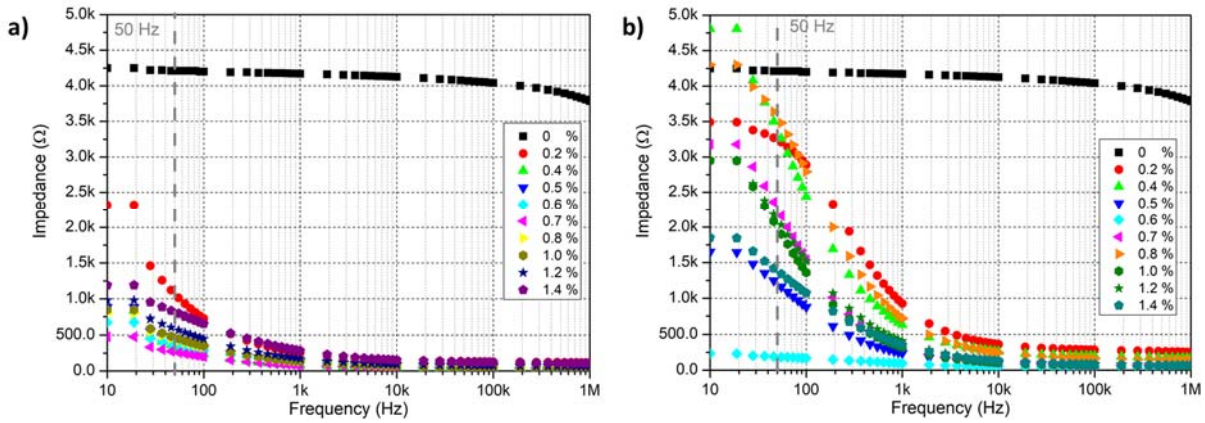
352 Figure 7. Presence of bunches in the CFRAN samples: a) CC mix and b) UHPC mix

353

354 4.2.2 Effect of C10/30 and CT12 fibres

355 In the case of C10/30 and CT12 fibres, the general electrical patterns obtained are similar to
356 those observed for CFRAN fibres, as shown in Figure 8. Nevertheless, an inversion
357 phenomenon is observed for both types of fibres. The incorporation of both types of rCFs
358 reduces the impedance of the samples until the rCF content of 0.4–0.5% is reached. Further
359 increases in the rCF content produce an inversion phenomenon and the impedance values
360 increase again. In the case of C10/30 fibres (Figure 8a), the maximum impedance reduction is
361 achieved for 0.5% content of rCF; a further increase in the rCF content results in a slight
362 increase in the measured impedance. The CT12 fibres exhibit a more evident inversion
363 phenomenon for rCF contents larger than 0.6% (see Figure 8b). These inversion phenomena
364 clearly highlight the inadequate dispersion of rCF in the concrete samples.

365

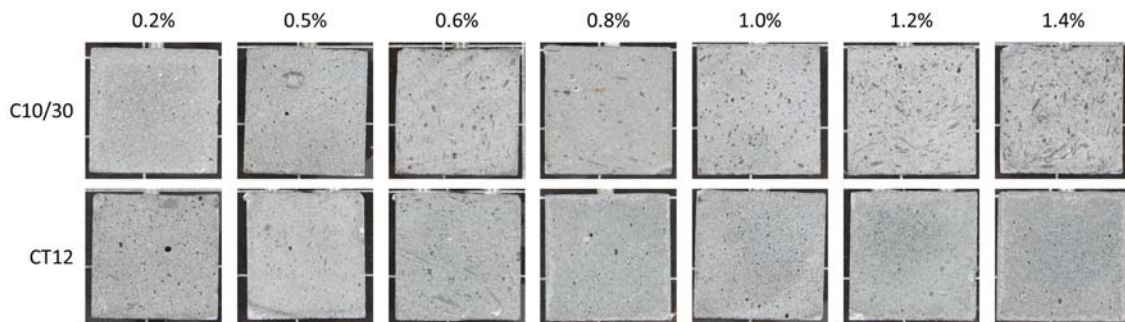


366

367 Figure 8. Bode diagrams for UHPC mixes with: a) C10/30 fibres and b) CT12 fibres

368

369 The visual inspection of the cross-section of the samples (Figure 9) also shows the presence
 370 of bunches of rCF. The distribution of rCF in the C10/30 concrete samples correlates with the
 371 impedance variation shown in Figure 8a. The number of fibres in the cross section increases
 372 up to a content of 0.6% of rCF. Bunches of rCF are observed in the cross section as the rCF
 373 content increases. The distribution of rCF in the CT12 samples presents some differences.
 374 The agglomerations of carbon fibres are observed for low contents of rCF. Nevertheless, for
 375 rCF contents larger than 0.6% no evidence of rCF can be detected in the cross section of the
 376 samples. The CT12 carbon fibres were provided as fibrillated sheets. A possible explanation
 377 for this result is the separation of the rCF sheets into individual carbon fibres or the
 378 degradation of the carbon fibres. The impedance variation for these samples (Figure 8b) may
 379 also be in accordance with a deterioration of the carbon fibres.



380

381 Figure 9. rCF dispersion in C10/30 and CT12 concrete samples

382

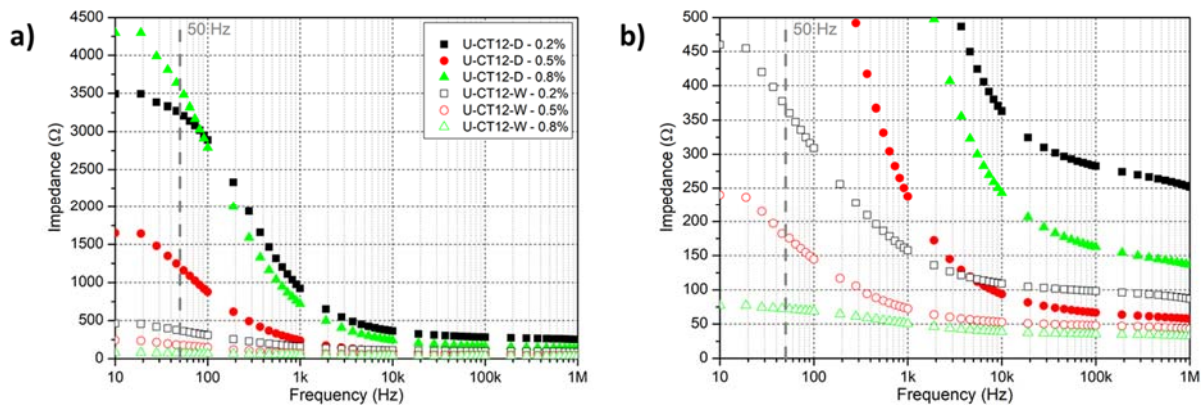
383 **4.2.3 Influence of rCF mixing method**

384 Notably, all the electrical patterns shown above correspond to rCF added to the dry mix after
385 the cement and aggregates. The effect of the mixing method on the electrical patterns is
386 illustrated in Figure 10. The incorporation of rCF into the wet mix after incorporating the
387 water and additives modifies the electrical behaviour of the samples significantly. The
388 modification affects both the impedance value and the frequency at which the impedance
389 stabilises. First, the impedance of the samples is drastically reduced when the mixing method
390 is modified. Furthermore, no inversion effect appears in the samples in the wet mix, thus
391 demonstrating good dispersion of the rCF into the cementitious matrix. The presence of
392 bunches of rCF could not be observed in the analysis of the cross-section of the concrete
393 samples (see Figure 11). Furthermore, no evidence of fibre deterioration is observed in the
394 cross section of CT12 concrete samples.

395

396 Figure 12 illustrates the variation of Z_{CT12-D}/Z_{CT12-W} ratio with the frequency that helps to
397 identify the effect of the mixing method on the dispersion of rCF in the cementitious matrix.
398 For rCF contents below the percolation threshold (rCF contents of 0.2 and 0.5%), the
399 influence of fibre dispersion results in a difference in impedance of the order of ten times.
400 Nevertheless, when the rCF is approximately equal to or more than the percolation threshold
401 (rCF content of 0.8%), the better fibre dispersion in the wet mix samples facilitates larger
402 differences in the electrical behaviour of the samples. Notably, once the frequency surpasses
403 the C_f value, the ratio Z_{CT12-D}/Z_{CT12-W} stabilises at an average value of 3. Second, the
404 incorporation of the rCF into the wet mix also reduces the value of C_f for different concrete
405 samples to approximately 100 kHz for the dry mix samples and 1 kHz for the wet mix
406 samples.

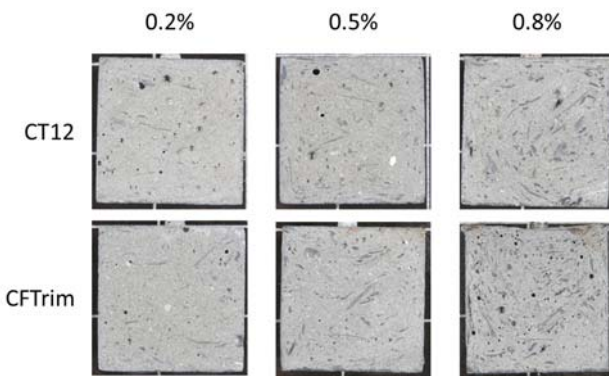
407



408

409 Figure 10. Effect of the mixing method on the electrical pattern of CT12 mixes: a) complete
410 impedance scale and b) zoom-in the 0–500 Ω range of impedance

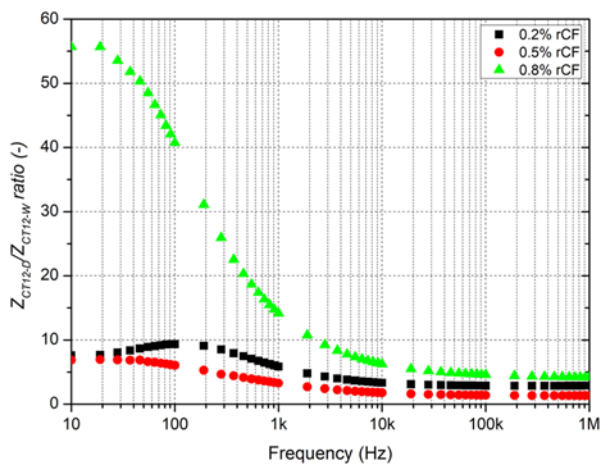
411



412

413 Figure 11. rCF dispersion in wet mix concrete samples

414

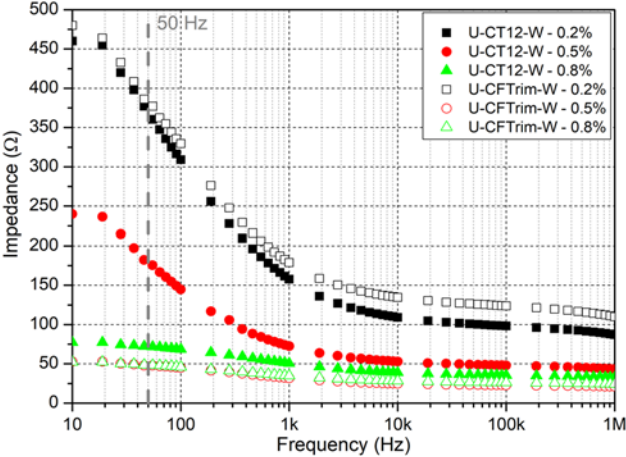


415

416 Figure 12. Variation of Z_{CT12-D}/Z_{CT12-W} ratio with frequency

417
418
419
420
421
422
423
424
425
426
427

Furthermore, the incorporation of the rCF into the wet mix also facilitates the comparison between the electrical patterns of CT12 and CFTrim (see Figure 13). Although CT12 and CFTrim rCFs exhibit different electrical properties (see Table 2), the electrical behaviours of their equivalent concrete samples are quite similar. For rCF content of 0.8%, the percolation threshold value is reached and a continuous network of rCFs is formed in accordance with the previous studies (51). The similarities observed between the electrical patterns of CT12 and CFTrim concrete samples demonstrate that the electrical resistivity is determinate at the end by the cementitious paste that surrounds the rCF rather than by the electrical resistivity of the later.



428
429
430
431
432
433
434
435
436

Figure 13. Comparison of the electrical behaviour of UHPC mixes with CT12 and CFTrim fibres added to the wet mix

4.2.4 Electrical resistivity calculation

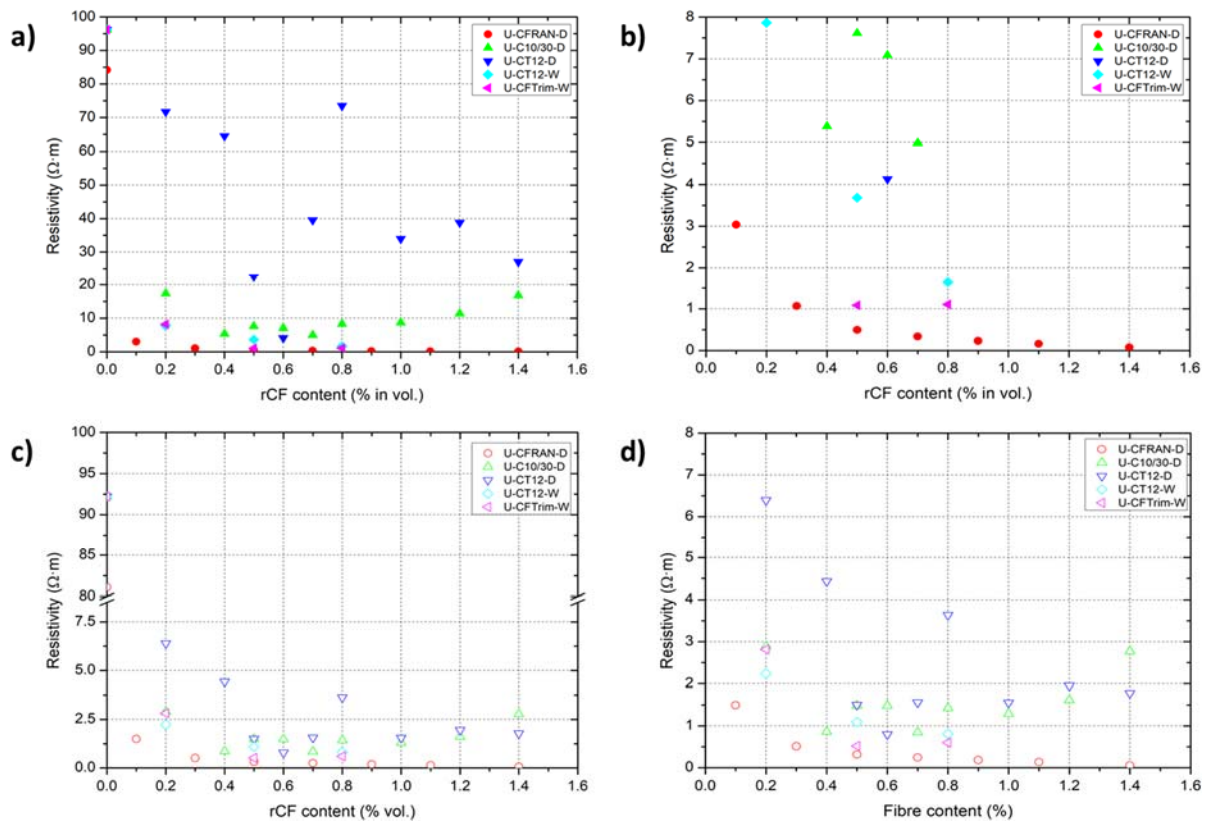
The electrical resistivity of different concrete samples can be calculated from the measured impedance. The impedance measured, Z , is a complex number and thus cannot be used to determine the electrical resistivity of the samples. The electrical resistance is used instead, as described by equation [5]. As AC measurements were obtained at different frequencies, a

437 non-trivial question is to determine the frequency at which the electrical resistivity must be
438 calculated. Many authors achieved the AC characterization of carbon fibre-reinforced
439 concrete (17,50,52) but the authors only found one reference that provided the nominal
440 frequency at which the electrical resistivity was calculated. Chen et al. (51) chose 100 kHz as
441 the value of C_t in their experiments. Therefore, in this work, two electrical resistivity values
442 are obtained: $\rho_{50\text{ Hz}}$ and $\rho_{100\text{ kHz}}$. As stated previously, $\rho_{50\text{ Hz}}$ is of high technical importance as
443 the standard frequency for AC is 50 Hz.

444

445 The frequency selected for the electrical resistivity measurements affects the electrical
446 resistivity values as shown in Figure 14. The measurements obtained at 50 Hz clearly
447 demonstrate the influence of the fibre dispersion on the electrical resistivity of the samples
448 (see Figure 14a and b). This situation was clearly observed with U-CT12-D samples. These
449 samples exhibited inadequate dispersion of the fibres and bunches appeared after the visual
450 inspection. This was also reflected in $\rho_{50\text{ Hz}}$ as they exhibited larger electrical resistivity
451 values. Nevertheless, the electrical resistivity of these samples measured at 100 kHz is
452 approximately 1.5 $\Omega\cdot\text{m}$. The lowest electrical resistivity is obtained for the wet mix rCF
453 samples (U-CT12-W and U-CFTrim-W). Furthermore, these samples are the ones less
454 affected by the chosen frequency owing to the good dispersion of fibres in the cementitious
455 matrix. The values of $\rho_{50\text{ Hz}}$ obtained for the wet mix rCF samples are in the range of 3 to 0.6
456 $\Omega\cdot\text{m}$, which is consistent with the reported values for virgin carbon fibres (22,51,52).

457



458

459 Figure 14. Electrical resistivity variation with the rCF content of different concrete samples

460 obtained at 50 Hz (a and b) and 100 kHz (c and d)

461

462 4.2.5 Estimation of C_t

463 In the different samples analysed, we have identified a ‘cut-off’ frequency: the *capacitance*

464 *threshold*, C_t . For frequency values between 10 Hz and C_t , there is a large variation in the

465 impedance of the samples. For frequency values above C_t , the impedance reaches a plateau

466 and stabilises. The values of C_t vary in the range of 1 to 100 kHz depending on the type and

467 content of fibre and the mixing method. The complex impedance spectra (Nyquist diagrams)

468 of different concrete samples will be analysed to understand this question more clearly. The

469 Nyquist diagrams of cementitious materials with conductive inclusions normally exhibit three

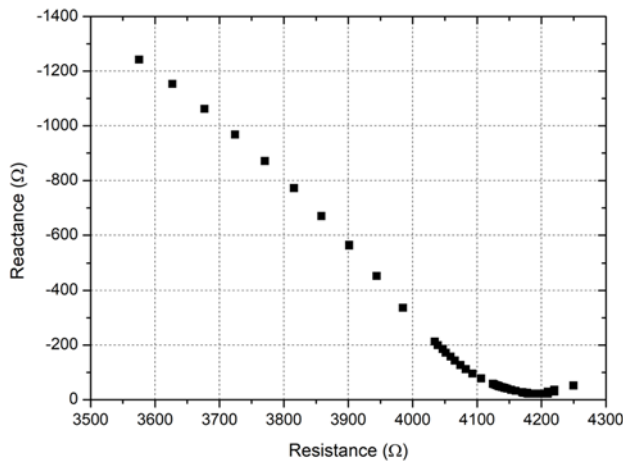
470 individual arc/features, accounting for the electrochemical reactions and product layer

471 deposition at the electrodes and bulk-related features (53). Figure 15 illustrates the Nyquist

472 diagram for the neat UHPC concrete sample in which only two arcs can be observed. The

473 spur element on the right side is related to the polarisation effects at the electrode (54). The
474 rest of the diagram is part of the arc related to the bulk response of the sample. The
475 incorporation of the rCF modifies the diagram as shown in Figure 16. Both the reactance and
476 electrical resistance values decrease and the feature attributed to the electrode polarization
477 effects is not discernible, as described by previous researchers (54). Ford et al. (53)
478 demonstrated that the Nyquist diagram of cementitious samples is affected by the inclusion of
479 conductive phases. The emerging high-frequency arc that appears on the left side of the
480 diagram is related to the bulk features of the sample. The other arc is characteristic of the
481 conductive fibres (53,55).

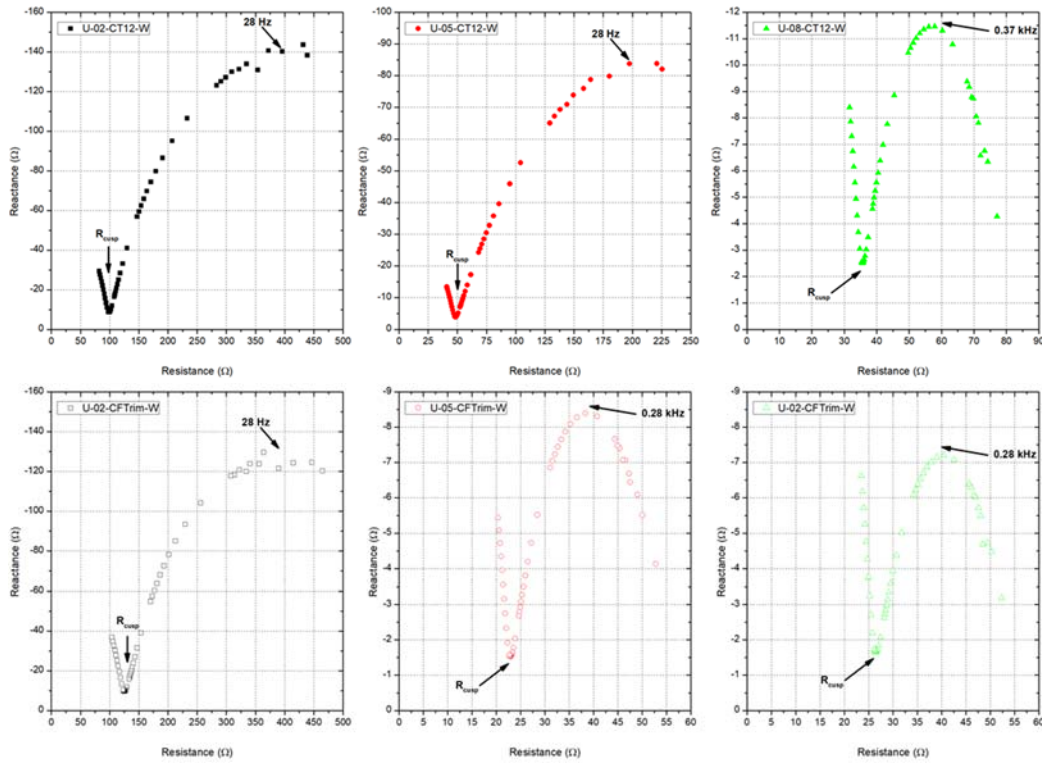
482



483

484 Figure 15. Nyquist diagram for the reference UHPC concrete

485



486

487 Figure 16. Nyquist diagrams for the UHPC concretes with rCF fibers added to the wet mix

488

489 The Nyquist diagrams can also account for the rCF dispersion on the cementitious matrix as

490 shown in Figure 17. The incorporation of CT12 fibers into the dry mix results in large

491 increases in both the reactance and electrical resistance as compared with the wet mix samples

492 (see Figure 16). Furthermore, the inversion phenomena caused by the build-up of the rCF is

493 also evidenced. Two parameters can be obtained from the Nyquist diagrams: the frequency of

494 the maximum of the arc (f_{max}), and the frequency and electrical resistance at the cusp-point

495 between two arcs (f_{cusp} , R_{cusp}) as presented in Table 3 for CT12 and CFTrim concrete samples.

496 The values of f_{max} are very similar for different samples and vary between 28 Hz and 370 Hz,

497 and are related to the rCF inclusion in the cementitious matrix. The analysis of the

498 characteristic values of the cusp-point is also of interest. Mason et al. identified the *cusp*

499 *frequency* (f_{cusp}) as the frequency value required to bypass the cementitious matrix that

500 surrounds the rCF (56). There is a clear shift of the cusp electrical resistance as the rCF

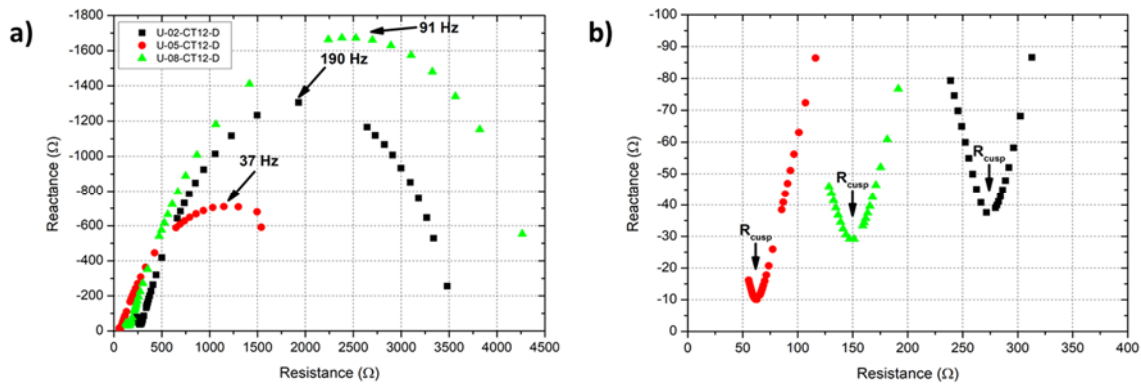
501 increases. The reduction in R_{cusp} corresponds to the reduction in the outer bulk contributions

502 to the fibre current path. Furthermore, the values obtained for f_{cusp} are very close to those
 503 indicated as the *capacitance threshold* (C_t). C_t can be estimated from the reactance value at
 504 the cusp-point according to equation [6].

505

$$506 \quad C_t = \frac{1}{2 \cdot \pi \cdot f_{cusp} \cdot X_{cusp}} \quad [6]$$

507



508

509 Figure 17. Nyquist diagrams for the UHPC concretes with CT12 fibres added to the dry mix

510

511 Table 3. Parameters obtained from the Nyquist diagrams of CT12 and CFTrim concrete

512 samples

| Sample | rCF content (% in vol.) | Parameter | | | |
|------------|----------------------------|----------------|-------------------------|-----------------|------------|
| | | f_{max} (Hz) | R_{cusp} (Ω) | f_{cusp} (Hz) | C_t (nF) |
| U-CT12-D | 0.2 | 190 | 271.6 | 190 kHz | 22.3 |
| | 0.5 | 37 | 62.9 | | 82.6 |
| | 0.8 | 91 | 151.3 | | 28.7 |
| U-CT12-W | 0.2 | 28 | 99.2 | 64 kHz | 284.7 |
| | 0.5 | 28 | 48.5 | | 637.2 |
| | 0.8 | 370 | 35.6 | 73 kHz | 868.2 |
| U-CFTrim-W | 0.2 | 37 | 125.4 | 55 kHz | 301.9 |
| | 0.5 | 280 | 22.9 | 64 kHz | 1629.3 |
| | 0.8 | 280 | 26.4 | | 1508.2 |

513

514

515 The values obtained for C_t can be related to the ‘*frequency switchable model*’ described by
516 several authors (55–57). Therefore, the *capacitance threshold* can be related to the
517 cementitious paste that coats the carbon fibres. Two adjacent carbon fibres will always be
518 surrounded by cementitious paste. This situation can be simplified and consider the system of
519 the carbon fibres and the cementitious paste equivalent to a parallel-plate capacitor with its
520 capacitance C defined by equation [7], where ε is the permittivity, A is the area of the plates,
521 and d the distance between them. If ε and A are assumed constant values, reductions in the
522 distance between the plates produce an increase in the capacitance value of the system

523

$$524 \quad C = \frac{\varepsilon \cdot A}{d} \quad [7]$$

525

526 Consequently, as the rCF content increases and the dispersion of carbon fibres is enhanced,
527 the distance between the fibres is reduced, as reflected by the increasing C_t values shown in
528 Table 3. Finally, the overall electrical resistance of the concrete sample is reduced.

529

530 **5. Conclusions**

531 This paper has demonstrated the possibility of developing conductive cementitious materials
532 with recycled carbon fibres. This research facilitates the incorporation of multifunctional
533 cementitious materials in the civil engineering industry, as the cost of the rCF is much lower
534 than that of previously used carbonaceous materials. Thus, the use of multifunctional
535 cementitious materials can be extended in actual concrete structures and not only in laboratory
536 and small scale test applications.

537

538

539 Four different types of rCF were evaluated in this work. The best dispersion of the rCF was
540 achieved for the fibrillated samples with the length of 12 mm (CT12 and CFTrim). The
541 workability of the fresh concrete samples was significantly modified by the incorporation of
542 the rCF, although acceptable values were obtained for the concrete samples that incorporated
543 the rCF using the wet mix method. In terms of the mechanical performance, a reduction in
544 both flexural and compressive strength was observed with the adding of the rCF using the dry
545 mix method.

546

547 The electrical behaviours of different concrete samples with rCF did not differ significantly
548 from the electrical characteristics described in the literature for concrete samples with virgin
549 carbon fibres. The Bode diagrams of different concrete samples exhibited a common pattern.
550 The impedance of the samples decreased as the frequency increased up to a threshold value
551 and thereafter stabilised in a plateau. This frequency is sensitive to the fibre dispersion and is
552 required to bypass the cementitious matrix that surrounds the rCF. The electrical resistivity
553 values obtained for the wet mix rCF samples were between 3 and 0.6 $\Omega \cdot m$, which is
554 consistent with the reported values for virgin carbon fibres.

555

556 Furthermore, we have evaluated in this work presence of a *capacitance threshold* value (C_t) in
557 conductive cementitious materials. that is related with the cementitious paste that coats the
558 carbon fibres.

559

560 Lastly, the results presented in this article may also help boost the recycling industry of
561 carbon fibre composites, providing new added-value applications that may be used in large
562 structures. We are facing a world-wide problem on the recycle of obsolete aircrafts that are
563 actually been stored in large airfields. The incorporation of rCF in multifunctional concrete

564 structures may be good contribution and will allow to enhance the sustainability of our
565 infrastructures.

566

567 Furthermore,

568

569 **Acknowledgements**

570 The authors acknowledge the financial support provided by the Spanish Ministry of Economy
571 and Competitiveness through Project BIA2016-78742-C2-1-R, and the Torres Quevedo
572 Program (postdoctoral fellowships PTQ-14-07072 and PTQ-15-07562), as well as the support
573 from the Catalan Government through the Industrial Doctorate program DI-2015-013.

574 Furthermore, the authors wish to thank the company Escofet 1886 for their collaboration and
575 support throughout the project.

576

577 **References**

- 578 1. The Economist. Building works: An historic opportunity to improve infrastructure on
579 the cheap is in danger of being squandered. The Economist [Internet]. 2015; Available
580 from: [https://www.economist.com/news/finance-and-economics/21662593-historic-](https://www.economist.com/news/finance-and-economics/21662593-historic-opportunity-improve-infrastructure-cheap-danger)
581 [opportunity-improve-infrastructure-cheap-danger](https://www.economist.com/news/finance-and-economics/21662593-historic-opportunity-improve-infrastructure-cheap-danger)
- 582 2. European Innovation Partnership on Smart Cities and Communities. Strategic
583 Implementation Plan [Internet]. 2013. Available from:
584 http://ec.europa.eu/eip/smartcities/files/sip_final_en.pdf
- 585 3. Salonitis K, Pandremenos J, Paralikas J, Chryssolouris G. Multifunctional materials:
586 Engineering applications and processing challenges. Int J Adv Manuf Technol.
587 2010;49(5–8):803–26.
- 588 4. Khadilkar D. Energy-Harvesting Street Tiles Generate Power from Pavement Pounder

- 589 - Scientific American. Scientific American [Internet]. 2013 Apr [cited 2017 Aug 19];
590 Available from: [https://www.scientificamerican.com/article/pavement-pounders-at-](https://www.scientificamerican.com/article/pavement-pounders-at-paris-marathon-generate-power/)
591 [paris-marathon-generate-power/](https://www.scientificamerican.com/article/pavement-pounders-at-paris-marathon-generate-power/)
- 592 5. De Muynck W, De Belie N, Verstraete W. Microbial carbonate precipitation in
593 construction materials: A review. *Ecol Eng.* 2010;36(2):118–36.
- 594 6. Wiktor V, Jonkers HM. Field performance of bacteria-based repair system: Pilot study
595 in a parking garage. *Case Stud Constr Mater.* 2015;2:11–7.
- 596 7. Manso S, De Muynck W, Segura I, Aguado A, Steppe K, Boon N, et al. Bioreceptivity
597 evaluation of cementitious materials designed to stimulate biological growth. *Sci Total*
598 *Environ.* 2014;481(1):232–41.
- 599 8. Manso S, Mestres G, Ginebra MP, De Belie N, Segura I, Aguado A. Development of a
600 low pH cementitious material to enlarge bioreceptivity. *Constr Build Mater.*
601 2014;54:485–95.
- 602 9. Vaquero JM, Cugat V, Segura I, Calvo-Torrás MA, Aguado A. Development and
603 experimental validation of an overlay mortar with biocide activity. *Cem Concr*
604 *Compos.* 2016;74:109–19.
- 605 10. Chen PW, Chung DDL. Concrete as a new strain/stress sensor. *Compos Part B Eng.*
606 1996;27(1):11–23.
- 607 11. Shi ZQ, Chung DDL. Carbon fiber-reinforced concrete for traffic monitoring and
608 weighing in motion. *Cem Concr Res.* 1999;29(3):435–9.
- 609 12. Chung DDL. Cement-matrix composites for smart structures. Vol. 9, *Smart Materials*
610 *and Structures.* 2000. p. 389–401.
- 611 13. Chung DDL. Cement reinforced with short carbon fibers: A multifunctional material.
612 *Compos Part B Eng.* 2000;31(6–7):511–26.
- 613 14. Chung DDL. Carbon materials for structural self-sensing, electromagnetic shielding

- 614 and thermal interfacing. *Carbon N Y* [Internet]. 2012;50(9):3342–53. Available from:
615 <http://dx.doi.org/10.1016/j.carbon.2012.01.031>
- 616 15. Liu X, Wu S. Carbon Nanotube Based Self-sensing Concrete for Pavement Structural
617 Health Monitoring. Report_University of Minesota. 2012;7(4).
- 618 16. Ding Y, Chen Z, Han Z, Zhang Y, Pacheco-Torgal F. Nano-carbon black and carbon
619 fiber as conductive materials for the diagnosing of the damage of concrete beam.
620 *Constr Build Mater* [Internet]. 2013;43:233–41. Available from:
621 <http://dx.doi.org/10.1016/j.conbuildmat.2013.02.010>
- 622 17. Gomis J, Galao O, Gomis V, Zornoza E, Garcés P. Self-heating and deicing conductive
623 cement. Experimental study and modeling. *Constr Build Mater*. 2015;75:442–9.
- 624 18. Ding Y, Huang Y, Zhang Y, Jalali S, Aguiar JB. Self-monitoring of freeze-thaw
625 damage using triphasic electric conductive concrete. *Constr Build Mater*.
626 2015;101:440–6.
- 627 19. Zornoza E, Catalá G, Jiménez F, Andi6n LG, Garcés P. Electromagnetic interference
628 shielding with Portland cement paste containing carbon materials and processed fly
629 ash. *Mater Constr* [Internet]. 2010;60(300):21–32. Available from:
630 <http://materconstrucc.revistas.csic.es/index.php/materconstrucc/article/view/605/652>
- 631 20. Micheli D, Vricella A, Pastore R, Delfini A, Bueno Morles R, Marchetti M, et al.
632 Electromagnetic properties of carbon nanotube reinforced concrete composites for
633 frequency selective shielding structures. *Constr Build Mater*. 2017;131:267–77.
- 634 21. Lai Y, Liu Y, Ma D. Automatically melting snow on airport cement concrete pavement
635 with carbon fiber grille. *Cold Reg Sci Technol* [Internet]. 2014;103:57–62. Available
636 from: <http://www.sciencedirect.com/science/article/pii/S0165232X14000639>
- 637 22. Galao O, Ba6n6n L, Baeza F, Carmona J, Garcés P, Baeza JF, et al. Highly Conductive
638 Carbon Fiber Reinforced Concrete for Icing Prevention and Curing. *Materials* (Basel).

- 639 2016;9(4):281.
- 640 23. Wu J, Liu J, Yang F. Three-phase composite conductive concrete for pavement
641 deicing. *Constr Build Mater*. 2015;75:129–35.
- 642 24. Jing X, Wu Y. Electrochemical studies on the performance of conductive overlay
643 material in cathodic protection of reinforced concrete. *Constr Build Mater* [Internet].
644 2011;25(5):2655–62. Available from:
645 <http://dx.doi.org/10.1016/j.conbuildmat.2010.12.015>
- 646 25. Carmona J, Garcés P, Climent MA. Efficiency of a conductive cement-based anodic
647 system for the application of cathodic protection, cathodic prevention and
648 electrochemical chloride extraction to control corrosion in reinforced concrete
649 structures. *Corros Sci*. 2015;96:102–11.
- 650 26. Cañón A, Garcés P, Climent MA, Carmona J, Zornoza E. Feasibility of
651 electrochemical chloride extraction from structural reinforced concrete using a sprayed
652 conductive graphite powder-cement paste as anode. *Corros Sci*. 2013;77:128–34.
- 653 27. Han B, Ding S, Yu X. Intrinsic self-sensing concrete and structures: A review. *Meas J*
654 *Int Meas Confed* [Internet]. 2015;59:110–28. Available from:
655 <http://dx.doi.org/10.1016/j.measurement.2014.09.048>
- 656 28. Bai YH, Chen W, Chen B, Tu R. Research on electrically conductive concrete with
657 double-layered stainless steel fibers for pavement deicing. *ACI Mater J*.
658 2017;114(6):935–43.
- 659 29. Yoo D-Y, You I, Lee S-J. Electrical Properties of Cement-Based Composites with
660 Carbon Nanotubes, Graphene, and Graphite Nanofibers. *Sensors* [Internet].
661 2017;17(5):1064. Available from: <http://www.mdpi.com/1424-8220/17/5/1064>
- 662 30. Heymsfield E, Osweiler AB, Panneer Selvam R, Kuss M. Feasibility of Anti-Icing
663 Airfield Pavements Using Conductive Concrete and Renewable Solar Energy. 2013.

- 664 31. Pimenta S, Pinho ST. Recycling carbon fibre reinforced polymers for structural
665 applications: Technology review and market outlook. *Waste Manag* [Internet].
666 2011;31(2):378–92. Available from: <http://dx.doi.org/10.1016/j.wasman.2010.09.019>
- 667 32. Pickering SJ. Recycling technologies for thermoset composite materials — current
668 status. *Compos Part A Appl Sci Manuf*. 2006;37:1206–15.
- 669 33. Pimenta S, Pinho ST. Recycling carbon fibre reinforced polymers for structural
670 applications: Technology review and market outlook. *Waste Manag* [Internet]. 2011
671 Feb [cited 2017 Aug 19];31(2):378–92. Available from:
672 <http://linkinghub.elsevier.com/retrieve/pii/S0956053X10004976>
- 673 34. Wong KH, Pickering SJ, Rudd CD. Recycled carbon fibre reinforced polymer
674 composite for electromagnetic interference shielding. *Compos Part A Appl Sci Manuf*
675 [Internet]. 2010;41(6):693–702. Available from:
676 <http://dx.doi.org/10.1016/j.compositesa.2010.01.012>
- 677 35. Turner TA, Pickering SJ, Warrior NA. Development of recycled carbon fibre moulding
678 compounds - Preparation of waste composites. *Compos Part B Eng* [Internet].
679 2011;42(3):517–25. Available from:
680 <http://dx.doi.org/10.1016/j.compositesb.2010.11.010>
- 681 36. Akonda MH, Lawrence CA, EL-Dessouky HM. Electrically conductive recycled
682 carbon fibre-reinforced thermoplastic composites. *J Thermoplast Compos Mater*
683 [Internet]. 2013 Nov 21;28(11):1550–63. Available from:
684 <http://dx.doi.org/10.1177/0892705713513294>
- 685 37. Nguyen H, Fujii T, Okubo K, Carvellu V. Cement Mortar Reinforced with Recycled
686 Carbon Fibre and CFRP Waste. In: 17th European Conference on Composite
687 Materials, [Internet]. Munich: European Society for Composite Materials; 2016.
688 Available from:

- 689 https://www.researchgate.net/publication/309733808_Cement_Mortar_Reinforced_wit
690 [h_Recycled_Carbon_Fibre_and_CFRP_Waste](https://www.researchgate.net/publication/309733808_Cement_Mortar_Reinforced_wit)
- 691 38. Nguyen H, Carvelli V, Fujii T, Okubo K. Cement mortar reinforced with reclaimed
692 carbon fibres, CFRP waste or prepreg carbon waste. *Constr Build Mater* [Internet].
693 2016 Nov [cited 2017 Aug 22];126:321–31. Available from:
694 <http://linkinghub.elsevier.com/retrieve/pii/S0950061816314805>
- 695 39. Wen S, Chung DDL. Model of piezoresistivity in carbon fiber cement. *Cem Concr Res*.
696 2006;36(10):1879–85.
- 697 40. Narayanan R, Darwish IYS. Use of Steel Fibers as Shear Reinforcement. *Struct J*
698 [Internet]. 1987;84(3):216–27. Available from:
699 [https://www.concrete.org/publications/internationalconcreteabstractsportal.aspx?m=det](https://www.concrete.org/publications/internationalconcreteabstractsportal.aspx?m=details&ID=2654)
700 [ails&ID=2654](https://www.concrete.org/publications/internationalconcreteabstractsportal.aspx?m=details&ID=2654)
- 701 41. AENOR. UNE-EN 196-1:2005 Methods of testing cement. Part I: Determination of
702 strength. 2005.
- 703 42. Gao J, Wang Z, Zhang T, Zhou L. Dispersion of carbon fibers in cement-based
704 composites with different mixing methods. *Constr Build Mater* [Internet].
705 2017;134:220–7. Available from: <http://dx.doi.org/10.1016/j.conbuildmat.2016.12.047>
- 706 43. Wang C, Li K-Z, Li H-J, Jiao G-S, Lu J, Hou D-S. Effect of carbon fiber dispersion on
707 the mechanical properties of carbon fiber-reinforced cement-based composites. *Mater*
708 *Sci Eng A* [Internet]. 2008 Jul 25 [cited 2017 Oct 10];487(1–2):52–7. Available from:
709 [http://www.sciencedirect.com/recursos.biblioteca.upc.edu/science/article/pii/S0921509](http://www.sciencedirect.com/recursos.biblioteca.upc.edu/science/article/pii/S0921509307016978?via%3Dihub)
710 [307016978?via%3Dihub](http://www.sciencedirect.com/recursos.biblioteca.upc.edu/science/article/pii/S0921509307016978?via%3Dihub)
- 711 44. AENOR. UNE-EN 1015-3:2000 Methods of test for mortar for masonry.
712 Determination of consistence of fresh mortar (by flow table). 2000.
- 713 45. Gersing E. Measurement of electrical impedance in organs measuring equipment for

- 714 research and clinical applications. *Biomed Tech.* 1991;36:6–11.
- 715 46. Wen S, Chung DDL. The role of electronic and ionic conduction in the electrical
716 conductivity of carbon fiber reinforced cement. *Carbon N Y.* 2006;44(11):2130–8.
- 717 47. Wen S, Chung DDL. Double percolation in the electrical conduction in carbon fiber
718 reinforced cement-based materials. *Carbon N Y.* 2007;45(2):263–7.
- 719 48. Yakhlaf M, Safiuddin M, Soudki KA. Properties of freshly mixed carbon fibre
720 reinforced self-consolidating concrete. *Constr Build Mater* [Internet]. 2013;46:224–31.
721 Available from: <http://dx.doi.org/10.1016/j.conbuildmat.2013.04.017>
- 722 49. Grünewald S. Performance-based design of self-compacting fibre reinforced concrete
723 [Internet]. Delft University Press; 2004 [cited 2017 Aug 21]. Available from:
724 [https://repository.tudelft.nl/islandora/object/uuid:07a817aa-cba1-4c93-bbed-](https://repository.tudelft.nl/islandora/object/uuid:07a817aa-cba1-4c93-bbed-40a5645cf0f1?collection=research)
725 [40a5645cf0f1?collection=research](https://repository.tudelft.nl/islandora/object/uuid:07a817aa-cba1-4c93-bbed-40a5645cf0f1?collection=research)
- 726 50. Han B, Zhang L, Zhang C, Wang Y, Yu X, Ou J. Reinforcement effect and mechanism
727 of carbon fibers to mechanical and electrically conductive properties of cement-based
728 materials. *Constr Build Mater* [Internet]. 2016 Oct 30;125:479–89. Available from:
729 <http://www.sciencedirect.com/science/article/pii/S0950061816313265>
- 730 51. Chen B, Wu K, Yao W. Conductivity of carbon fiber reinforced cement-based
731 composites. *Cem Concr Compos.* 2004;26(4):291–7.
- 732 52. Baeza FJ, Galao O, Zornoza E, Garc??s P. Effect of aspect ratio on strain sensing
733 capacity of carbon fiber reinforced cement composites. *Mater Des* [Internet].
734 2013;51:1085–94. Available from: <http://dx.doi.org/10.1016/j.matdes.2013.05.010>
- 735 53. Ford S., Shane J., Mason T. Assignment of features in impedance spectra of the
736 cement-paste/steel system. *Cem Concr Res.* 1998;28(12):1737–51.
- 737 54. McCarter WJ, Starrs G, Chrisp TM, Banfill PFG. Complex impedance and dielectric
738 dispersion in carbon fiber reinforced cement matrices. *J Am Ceram Soc.*

- 739 2009;92(7):1617–20.
- 740 55. Torrents JM, Mason TO, Garboczi EJ. Impedance spectra of fiber-reinforced cement-
741 based composites: A modeling approach. *Cem Concr Res.* 2000;30(4):585–92.
- 742 56. Mason TO, Campo MA, Hixson AD, Woo LY. Impedance spectroscopy of fiber-
743 reinforced cement composites. *Cem Concr Compos.* 2002;24(5):457–65.
- 744 57. Hixson AD, Woo LY, Campo MA, Mason TO. The origin of nonlinear current-voltage
745 behavior in fiber-reinforced cement composites. *Cem Concr Res.* 2003;33(6):835–40.
- 746